Contents lists available at ScienceDirect

# Journal of Advanced Research

journal homepage: www.elsevier.com/locate/jare



# Original Article

# Paeonol protects against doxorubicin-induced cardiotoxicity by promoting Mfn2-mediated mitochondrial fusion through activating the PKCE-Stat3 pathway



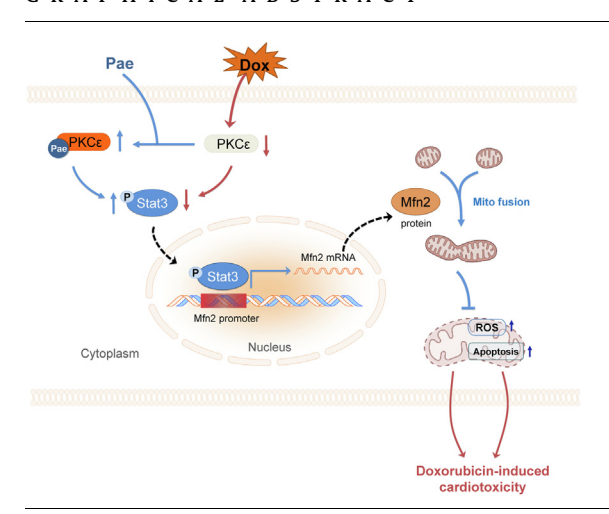
Mingge Ding a,b,c,1, Rui Shi c,d,1, Feng Fu d,1, Man Li d,e, Dema De c, Yanyan Du d,e, Zongfang Li a,b,\*

- a National & Local Joint Engineering Research Center of Biodiagnosis and Biotherapy, The Second Affiliated Hospital of Xi'an Jiaotong University, Xi'an, Shaanxi 710004, China
- b Center for Tumor and Immunology, the Precision Medical Institute, the Second Affiliated Hospital of Xi' an Jiaotong University, Xi'an, Shaanxi 710004, China
- Department of Geriatrics Cardiology, The Second Affiliated Hospital, School of Medicine, Xi'an Jiaotong University, Xi'an, Shaanxi 710004, China
- <sup>d</sup> Department of Physiology and Pathophysiology, Fourth Military Medical University, Xi'an, Shaanxi 710032, China
- <sup>e</sup> School of Life Science, Northwest University, Xi'an, Shaanxi, 710069, China

#### HIGHLIGHTS

- Paeonol promotes Mfn2-mediated mitochondrial fusion in doxorubicintreated hearts.
- Mfn2 knockdown or knockout blunts the protective effects of paeonol.
- Paeonol increases Mfn2 expression via Stat3-mediated transcription.
- Paeonol activates Stat3-Mfn2 signaling pathway via upregulating PKCε.
- Paeonol does not interfere with doxorubicin's antitumor efficacy.

## G R A P H I C A L A B S T R A C T



#### ARTICLE INFO

Article history: Received 22 April 2022 Revised 13 June 2022 Accepted 10 July 2022 Available online 14 July 2022

Keywords: Doxorubicin Paeonol Mitochondrial fusion PKCE Stat3

## ABSTRACT

Introduction: The anti-cancer medication doxorubicin (Dox) is largely restricted in clinical usage due to its significant cardiotoxicity. The only medication approved by the FDA for Dox-induced cardiotoxicity is dexrazoxane, while it may reduce the sensitivity of cancer cells to chemotherapy and is restricted for use. There is an urgent need for the development of safe and effective medicines to alleviate Dox-induced cardiotoxicity. Objectives: The objective of this study was to determine whether Paeonol (Pae) has the ability to protect against Dox-induced cardiotoxicity and if so, what are the underlying mechanisms involved.

Methods: Sprague-Dawley rats and primary cardiomyocytes were used to create Dox-induced cardiotoxicity models. Pae's effects on myocardial damage, mitochondrial function, mitochondrial dynamics and signaling pathways were studied using a range of experimental methods.

*Results*: Pae enhanced Mfn2-mediated mitochondrial fusion, restored mitochondrial function and cardiac performance both *in vivo* and *in vitro* under the Dox conditions. The protective properties of Pae were blunted

Peer review under responsibility of Cairo University.

<sup>\*</sup> Corresponding author at: National & Local Joint Engineering Research Center of Biodiagnosis and Biotherapy, The Second Affiliated Hospital of Xi'an Jiaotong University, China

E-mail address: lzf2568@mail.xjtu.edu.cn (Z. Li).

<sup>&</sup>lt;sup>1</sup> Mingge Ding, Rui Shi and Feng Fu contributed equally to this article.

Mfn2

when Mfn2 was knocked down or knocked out in Dox-induced cardiomyocytes and hearts respectively. Mechanistically, Pae promoted Mfn2-mediated mitochondria fusion by activating the transcription factor Stat3, which bound to the Mfn2 promoter in a direct manner and up-regulated its transcriptional expression. Furthermore, molecular docking, surface plasmon resonance and co-immunoprecipitation studies showed that Pae's direct target was PKCɛ, which interacted with Stat3 and enabled its phosphorylation and activation. Pae-induced Stat3 phosphorylation and Mfn2-mediated mitochondrial fusion were inhibited when PKCɛ was knocked down. Furthermore, Pae did not interfere with Dox's antitumor efficacy in several tumor cells

Conclusion: Pae protects the heart against Dox-induced damage by stimulating mitochondrial fusion via the PKCE-Stat3-Mfn2 pathway, indicating that Pae might be a promising therapeutic therapy for Dox-induced cardiotoxicity while maintaining Dox's anticancer activity.

© 2023 The Authors. Published by Elsevier B.V. on behalf of Cairo University. This is an open access article under the CC BY-NC-ND license (http://creativecommons.org/licenses/by-nc-nd/4.0/).

#### Introduction

Doxorubicin (Dox) is a representative drug of anthracycline antibiotics, which has significant efficacy and has been widely utilized to treat a wide range of tumor diseases, such as breast and ovarian cancer [1,2]. Although Dox possesses significant broadspectrum anticancer action, the cardiotoxic reactions caused by Dox therapy have become increasingly prominent. When Dox reaches a certain cumulative amount in vivo, it is easy to impair myocardial cells and eventually cause severe cardiotoxicity. The clinical manifestations can be irreversible cardiomyopathy and eventually heart failure, and the outcome could be fatal, which limits the clinical application of Dox [3,4]. Currently, the only FDAapproved compound for Dox-induced cardiotoxicity is dexrazoxane. Nevertheless, studies in chemotherapy-reveiving patients showed that dexrazoxane may reduce the sensitivity of cancer cells to chemotherapy and exacerbate myelosuppression, and was restricted by the FDA and EMA for use [5-7]. Hence, there is an urgent need for the development of safe and effective medicines to alleviate Dox-induced cardiotoxicity.

The heart is an organ that requires a lot of energy and is heavily reliant on mitochondrial function. Mitochondria provide most energy for the cardiomyocytes but also produce large amounts of reactive oxygen species (ROS) [8]. During the development of Dox-induced cardiomyopathy, increased mitochondrial ROS generation and subsequent mitochondrial dysfunction have been identified as key factors [9,10]. NADH or NADPH functions as an electron donor for Dox, leading to the production of a semiquinone radical. Semiquinone is re-oxidized in the presence of molecular oxygen to produce superoxide anion-free radicals, which can be transformed to other reactive oxygen species [11]. Moreover, studies have shown that an event that raises mitochondrial ROS generation and promotes mitochondrial dysfunction is abnormal morphology of mitochondria caused by unbalanced mitochondrial fusion/fission dynamics [12,13]. Mitochondrial fusion and fission are two opposing processes in regulating morphological alteration. Mitochondrial fusion refers to the joining of two or more healthy mitochondrial fragments to form a new enlarged mitochondrion, while mitochondrial fission refers to the fragmentation of the mitochondrion into tiny organelles [14]. According to the previous in vitro and in vivo evidences, Dox disrupts mitochondrial dynamics by suppressing mitochondrial fusion and accelerating mitochondrial fission in the hearts [15]. Balancing the mitochondrial dynamics attenuates ROS production and apoptosis. In contrast, mitochondrial fusion promotion has no effect on mitochondrial function in the hearts, while mitochondrial fission inhibition over a long period of time may compromise mitochondrial quality [16,17]. Promoting mitochondrial fusion appears to be a safer technique than inhibiting mitochondrial fission to preserve mitochondrial function in the hearts. Therefore, safe and efficient drugs that target the promotion of mitochondrial fusion may be of great therapeutic interest for Dox-induced cardiotoxicity. Currently, few studies have evaluated the effect of pharmacological therapies on Dox-induced cardiotoxicity from the aspect of promoting mitochondrial fusion.

Paeonol (Pae, chemically known as 2'-Hydroxy-4'-methoxyace topheone) is a natural phenol antioxidant extracted from Paeonia suffruticosa's root bark. Pae has been authorized for the treatment of inflammation and pain-related diseases by the FDA in China. Moreover, Pae has been demonstrated to inhibit ischemiainduced cardiomyocytes apoptosis via suppressing ROS [18,19] and protect mitochondria against glutamate-induced damage via maintaining mitochondrial membrane potential and inhibiting cytochrome c release [20], making it a potential pharmaceutical agent for cardiac and mitochondrial protection. Importantly, our previous study has found that Pae is a mitochondrial fusion promoter that prevents the development of diabetic cardiomyopathy [21]. Given the potential importance of mitochondrial fusion in Dox-treated hearts, we hypothesized that Pae might be effective in reducing Dox-induced cardiotoxicity via the promotion of mitochondrial fusion. Our findings show that Pae promotes Mfn2mediated mitochondrial fusion and reduces Dox-induced myocardial damage through the PKCE-Stat3 signaling pathway. Moreover, Pae did not interfere the anticancer activity of Dox in several tumor cells.

## **Materials and methods**

The Supplementary Materials and Methods section includes an expanded "Materials and Methods.".

## Ethics statement

All experiments involving animals were conducted according to the ethical policies and procedures approved by the ethics committee of the Xi'an Jiaotong University (Approval no. 2019–505, Xi'an, Shaanxi, China). All the studies in our experiments are conducted in compliance with the National Institutes of Health Guidelines for Use of Laboratory Animals (8th Edition, 2011).

## Cardiomyocytes isolation and culture

Pimary cardiomyocytes were isolated from 1 to 2 day old newborn Sprague-Dawley rats and incubated in DMEM with 10% FBS (Gibco, USA) [22]. Pae (MB1762; Dalian Meilun Biology Technology, China) was administrated to cardiomyocytes with or without Dox for 24 h [23].

#### Animals and treatment

Male 6–8-week-old Sprague-Dawley rats (weighing 220–250 g) in a specific pathogen-free (SPF) grade were obtained from Xi'an Jiaotong University and kept in standard temperature, humidity, and light conditions. A dosage of 5 mg/kg Dox (HY-15142; MCE, Shanghai, China) was administered intraperitoneally to the rats on days 1, 6 and 11 (3 times/2 weeks) [24,25]. The control animals received an equivalent amount of normal saline injection. According to the previous studies [26,27], Pae was mixed with the vehicle (0.5% sodium carboxymethyl cellulose) and then given to the animals through oral gastric gavage at 75, 150, or 300 mg/kg each day after the last Dox injection.

## Molecular docking

The binding affinity between Pae and PKCε was investigated using Autodock Vina Version 1.1.2. In brief, Pae's Mol2 file was downloaded from PubChem. AutoDock Tools was used to convert Mol2 file to PDBQT formant. The Protein Data Bank (PDB) provided the 3D crystal structure of the PKC C2 domain (PDB ID: 1GMI). The PKCε C2 domain's search grid was established with dimensions size\_x: 30, size\_y: 30, and size\_z: 30. The docking process was performed as described previously [28,29]. Moreover, PKCε activity was determined using the Promega PKCε Kinase Assay kit according to the manufacturer's instructions.

#### Binding analysis by surface plasmon resonance (SPR)

SPR analysis was carried out using a Biacore T200 instrument equipped with a CM5 sensor chip (BR-1005–30; Cytiva) to determinate protein-molecular interactions as previously described [30]. In brief, recombinant human PKCɛ protein was immobilized in CM5 sensor chip channels amine-coupling kit (BR100050; Cytiva). Dox or Pae was dissolved in PBS-P (28995084; Cytiva). Dox or Pae was delivered into the flow system in a series of concentrations for 120 s and followed by 120 s dissociation. The Biacore T200 Evaluation software was used to analyze the data. Based on the 1:1 Langmuir binding model, the equilibrium dissociation constant (Kd) was determined.

## Statistical analysis

All the data in the experiment are measurement data. The data fit into a normal distribution and are presented as the mean  $\pm$  SEM. GraphPad Prism 8.0 software was used for all statistical analyses. For more than two experimental groups at different time-points in Supplementary Figure S9 A–B, two-way repeated ANOVA with post-hoc Bonferroni's multiple comparison test was applied. For the data from more than two groups in the other Figures, one-way ANOVA with post-hoc Tukey's multiple comparison tests were used. P values of<0.05 (P < 0.05) were deemed statistically significant.

#### Results

Pae restored mitochondrial fusion and enhanced mitochondrial function in the Dox-treated cardiomyocytes

According to the previous study [31], the cardiomyocytes were administrated with various concentrations of Pae (12.5, 25, 50, 100  $\mu$ mol/L) in the absence or presence of Dox (3  $\mu$ mol/L) for 24 h. The CCK8 assay showed that Pae alone had no obvious cytotoxicity effect on the cardiomyocytes, and the most effective concentration of Pae regarding cell viability in the Dox-treated

cardiomyocytes was 50 µmol/L (Supplementary Fig. S1). Therefore, the concentration of Pae at 50 µmol/L was chosen in the following experiments. As shown in Fig. 1A and B, Pae (50 µmol/L) not only increased cell viability but also inhibited lactic dehydrogenase (LDH) release in the Dox-treated cardiomyocytes. A reduction in mitochondrial membrane potential is an early indicator of cell apoptosis [32]. TUNEL and JC-1 staining showed that increased cell apoptosis and decreased mitochondrial membrane potential  $(\Delta \psi m)$  were observed in Dox-treated cardiomyocytes compared to control cells (Fig. 1C-E and G). Both cellular ROS (green fluorescence) and mitochondria-derived ROS (red fluorescence) were significantly enhanced in Dox-treated cardiomyocytes (Fig. 1F, H and I). The overlapping staining (merged yellow fluorescence) of ROS indicated that most cellular ROS originated from mitochondria (Fig. 1F). Pae administration resulted in substantial reductions in the apoptosis and oxidative stress, as well as a considerable increase in mitochondrial membrane potential ( $\Delta \psi m$ ) (Fig. 1C-I).

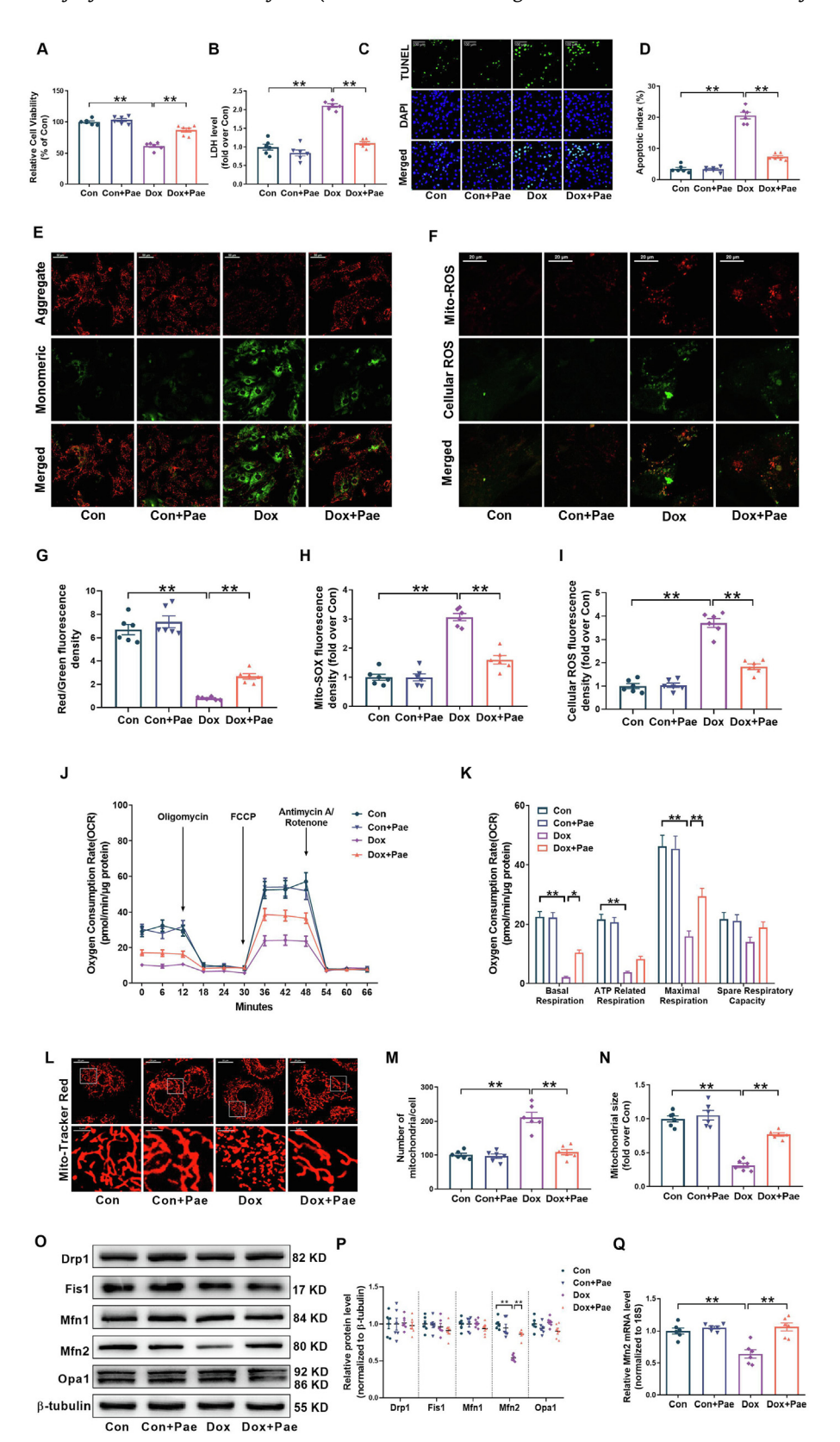
In addition, Dox insult inhibited the mitochondrial respiratory capacities including basal respiratory, ATP-related respiratory and maximal respiration (Fig. 1] and K). Pae partly recovered basal respiratory and maximal respiration capacities in the Dox-treated cardiomyocytes (Fig. 1] and K). Different from highly interconnected (elongated) mitochondria in control cardiomyocytes, mitochondria in the Dox-treated cardiomyocytes presented as round and smaller fragments. The mitochondrial size was reduced while the mitochondrial number per cell was elevated. Pae increased mitochondrial size while reducing mitochondrial number, indicating that Pae restored mitochondrial fusion in Dox-treated cardiomyocytes (Fig. 1L-N). Subsequently, the levels of key proteins involved in mitochondrial fission/fusion dynamics were determined. The protein expressions of Drp1, Fis1, Mfn1 and Opa1 did not alter significantly, only Mfn2 was downregulated following Dox stimulation (Fig. 10 and P), indicating that Dox inhibited Mfn2-mediated mitochondrial fusion in the cardiomyocytes. A downregulation of Mfn2 mRNA and pre-mRNA expressions were synchronously observed (Fig. 1Q and Supplementary Fig. S2A). Pae reversed the decrease in the protein and mRNA as well as pre-mRNA expressions of Mfn2 under the Dox conditions (Fig. 1-O-Q and Supplementary Fig. S2A). Moreover, Dox (3 μmol/L) significantly inhibited the luciferase activity of the Mfn2 promoter reporter, while Pae (50 µmol/L) enhanced the luciferase activity of the Mfn2 promoter reporter under the Dox conditions (Supplementary Fig. S2B). These data imply that Mfn2 expression may be modulated at the level of transcription. All the results collectively demonstrated that Pae administration elevated Mfn2 transcription and restored mitochondrial fusion and function in the Dox-treated cardiomyocytes.

# Pae administration alleviated Dox-induced cardiotoxicity in the

After demonstrating that Pae protected the cardiomyocytes against Dox-induced injury *in vitro*, Pae's protective properties were subsequently verified *in vivo*. The left ventricular ejection fraction (LVEF) and fractional shortening (LVFS) were both considerably decreased, while the LV end-systolic diameter (LVESD) was enlarged in the hearts of Dox-injected rats compared with those of control rats (Fig. 2A-D). Pae supplementation at the dose of 150 mg/kg/d or 300 mg/kg/d but not 75 mg/kg/d enhanced LVEF and LVFS while lowering LVESD in the Dox-treated rats (Fig. 2A-D). The left ventricular end-diastolic diameter (LVEDD) did not differ significantly across all the groups (Fig. 2A and E). Since the greatest efficacy was observed in the dose of 150 mg/kg/d Pae, this dose was deemed optimal and used in the subsequent animal studies, which was indicated as Con + Pae or Dox + Pae group. The cardioprotective effects of Pae at the dose of 150 mg/kg/d were further

validated by hemodynamic measurements and myocardial injury-related serum enzymes including lactic dehydrogenase (LDH) and creatine kinase isotype MB (CK-MB). It was shown in Fig. 2F-K that left ventricular systolic pressure (LVSP) and ± LV dp/dt max were significantly lowered, while left ventricular end diastolic pressure (LVEDP) and myocardial injury-related serum enzymes (LDH and

CK-MB) was elevated in Dox-treated rats compared with control animals. Pae administration elevated LVSP and ± LV dp/dt max while lowering LVEDP and myocardial injury-related serum enzymes in Dox-treated rats (Fig. 2F-K). All of these findings showed that Pae preserved cardiac function and effectively protected against Dox-induced cardiotoxicity.



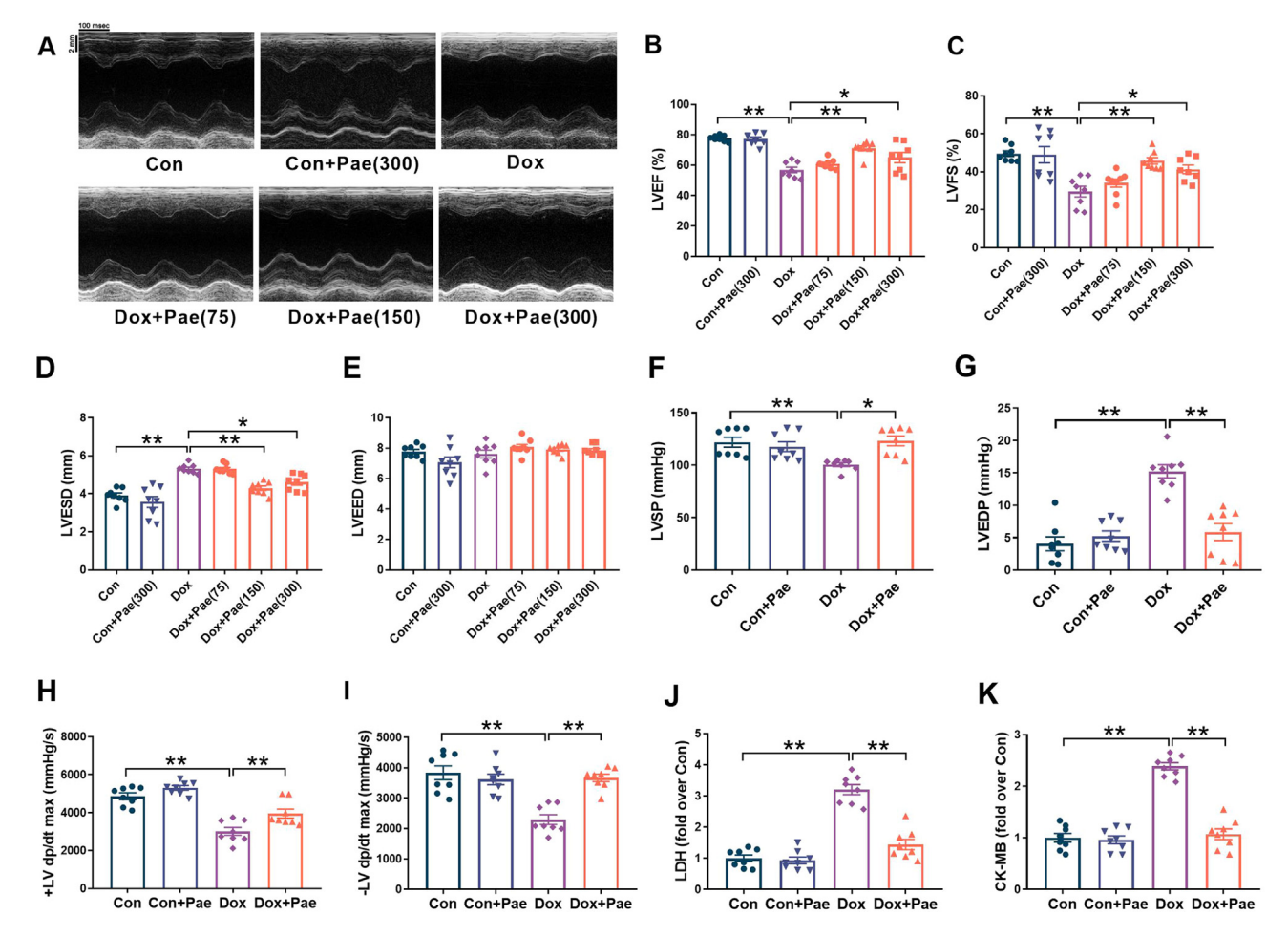


Fig. 2. Pae administration alleviated Dox-induced cardiotoxicity in the rats. (A) Representative images of M—mode echocardiography (Quantitative data are presented in B-E). (B) LVEF, left ventricular ejection fraction. (C) LVFS, left ventricular fractional shortening. (D) LVESD, left ventricular end-systolic diameter. (E) LVEDD, left ventricular end-diastolic diameter. (F) LVSP, left ventricular systolic pressure. (G) LVEDP, left ventricular end-diastolic pressure. (H-I) the maximal and minimal first derivative of LV pressure (±LV dP/dt<sub>max</sub>). (J) Plasma LDH level. (K) Plasma CK-MB level. n = 8 per group. \*P < 0.05, \*\*P < 0.01.

Pae administration improved cardiac structure and inhibited cardiomyocyte apoptosis as well as oxidative stress in the Dox-treated heart

Myocardial fibrosis and cardiac atrophy are significant features of Dox-induced myocardial injury [25,33]. Compared with control rats, Dox-treated rats had a higher collagen volume fraction and a lower heart weight (HW)/body weight (BW) ratio as well as a

Fig. 1. Pae restored mitochondrial fusion and enhanced mitochondrial function in the Dox-treated cardiomyocytes. (A) Relative cell viability. (B) Lactate dehydrogenase (LDH) release determined in cell supernatant. (C) Representative images of TUNEL and DAPI staining. (Quantitative data are presented in D). Original magnification × 200. (D) Quantitative data of the apoptotic index. (E) Representative images of mitochondrial membrane potential stained by JC-1. (Quantitative data are presented in G). Original magnification  $\times$  200. (F) Representative images of MitoSOX-stained mitochondrial ROS (red fluorescence) and DCFH-DA-stained cellular ROS production (green fluorescence). Original magnification × 600. (G) Quantification of mitochondrial membrane potential. (H) Quantitative data of relative mitochondrial ROS fluorescence density. (I) Quantitative data of relative whole-cell ROS fluorescence density. (J-K) Oxygen consumption rate (OCR) and quantitative data of OCR. (L) Representative MitoTracker Red-stained mitochondrial morphology images. Original magnification × 600. (M) Quantitative data of mitochondrial number per cell. (N) Quantitative data of mean mitochondrial size. (O-P) The mitochondrial fission/fusion-related proteins' representative blots and quantitative data. (Q) Quantitative data of Mfn2 mRNA expression. Dox, doxorubicin (3  $\mu$ mol/L); Pae, paeonol (50  $\mu$ mol/L). n = 6 per group. \*P < 0.05, \*\*P < 0.01. (For interpretation of the references to colour in this figure legend, the reader is referred to the web version of this article.)

lower heart weight (HW)/tibia length (TL) ratio (Supplementary Fig. S3A-C). Pae administration effectively reduced the structural abnormalities in the hearts caused by Dox (Supplementary Fig. S3A-C). The pathophysiology of Dox-induced cardiotoxicity has been associated with cardiomyocyte apoptosis and oxidative stress [34]. As expected, compared with the control hearts, Dox-treated hearts exhibited elevated myocardial apoptosis and oxidative stress (Supplementary Fig. S3D-L: apoptosis index, Bax expression, cleaved caspase 3 expression, DHE staining and MDA content were increased, while Bcl2 expression, GPx content, MnSOD expression were decreased.). Pae administration substantially reduced myocardial apoptosis and oxidative stress in the hearts upon Dox insult (Supplementary Fig. S3D-L).

Pae restored mitochondrial fusion and enhanced mitochondrial function in the Dox-treated hearts

The effects of Pae on mitochondrial fusion were further verified *in vivo*. Compared with the control hearts, Dox-treated hearts had smaller mitochondrial size (Fig. 3A and C). Moreover, Dox-treated hearts showed a higher percentage of mitochondria with a size < 0.6  $\mu m^2$ , and a low percentage of mitochondria with a size between 0.6  $\mu m^2$ –1  $\mu m^2$  or > 1  $\mu m^2$  (Fig. 3D). Consistent with the results *in vitro*, the protein and mRNA/pre-mRNA expressions of Mfn2 were similarly reduced in Dox-treated hearts compared to control hearts. (Fig. 3E–H). Pae restored mitochondrial fusion and the protein and mRNA/pre-mRNA levels of Mfn2 in the Dox-

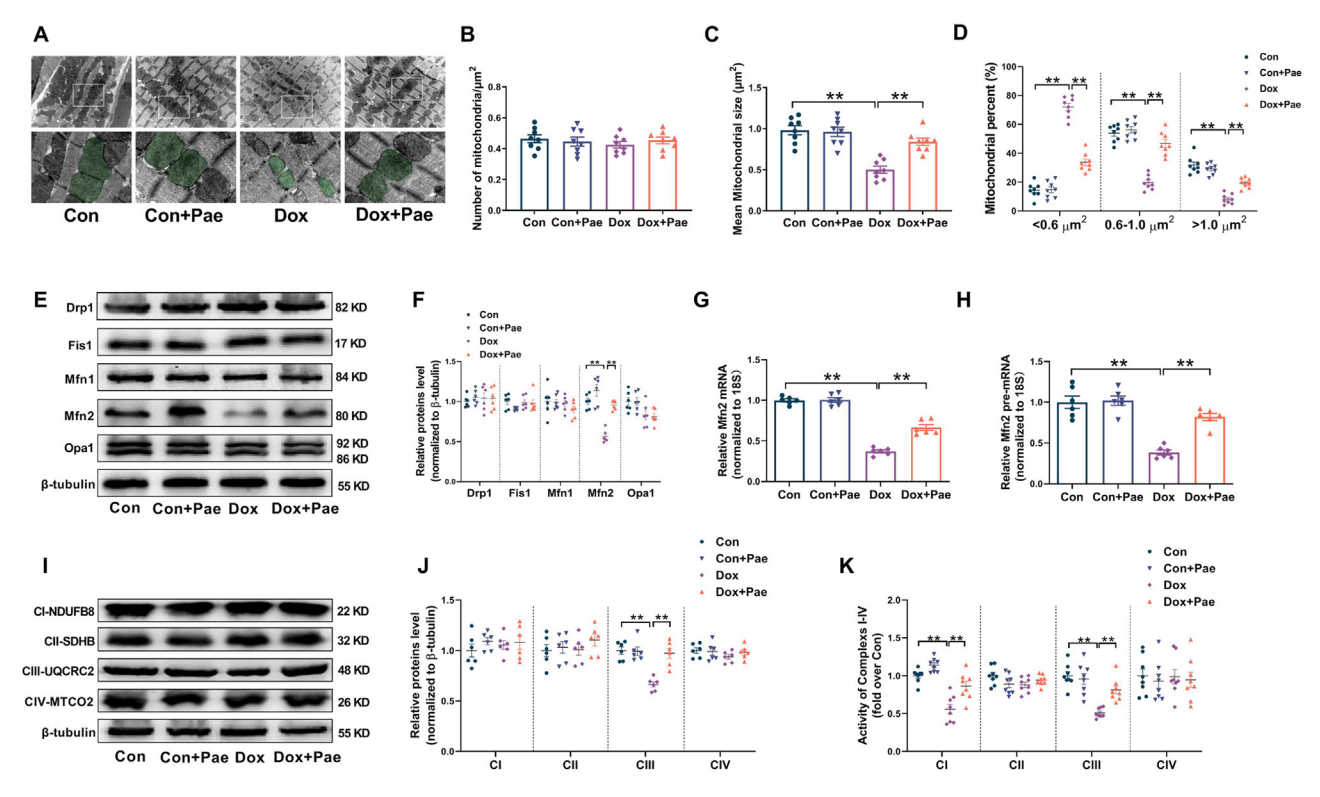


Fig. 3. Pae restored mitochondrial fusion and enhanced mitochondrial function in the Dox-treated hearts. (A) Representative mitochondrial images obtained by transmission electron microscope (Quantitative data are presented in B-D). Original magnification  $\times$  15000. Mitochondria were marked with light green. (B) Quantitative data of mitochondrial number per  $\mu$ m². (C) Quantitative data of mean mitochondrial size. (D) The proportion of mitochondria in a specific area categorized into three size groups (<0.6  $\mu$ m², within 0.6–1.0  $\mu$ m², > 1.0  $\mu$ m²) was counted. (E-F) The mitochondrial fission/fusion-related proteins' representative blots and quantitative data. (G) Quantitative data of Mfn2 pre-mRNA expression. (I-J) Representative blots and quantitative data of mitochondrial respiratory chain complex I-IV (CI-IV). (K) Quantitative data of mitochondrial complex I to IV (CI to CIV) activity. n = 8 per group for Fig. A-D and J and n = 6 per group for Fig. E-I. \*\*P < 0.01. (For interpretation of the references to colour in this figure legend, the reader is referred to the web version of this article.)

treated hearts (Fig. 3A-H). The abnormal changes in mitochondrial morphology are often associated with mitochondrial dysfunction [35]. The expression of Complex I was unchanged but its activity was significantly reduced after Dox insult (Fig. 3I-K). Both the expression and activity of Complex III were reduced in the Doxtreated hearts (Fig. 3I-K). Pae reversed the reduction in the expression of Complex III and the activity of complexes I, III in the Doxtreated hearts (Fig. 3I-K). These results demonstrated that Pae restored Mfn2-mediated mitochondrial fusion and alleviated mitochondrial dysfunction in the Dox-treated hearts.

Knockdown or knockout of Mfn2 blunted the cardioprotective properties of Pae under the Dox conditions

Whether the elevation of Mfn2 expression was essential for Pae's mitochondrial and cardiac protective effects was subsequently explored. Knockdown of Mfn2 with adenovirus encoding Mfn2 shRNA diminished the ability of Pae to enhance mitochondrial fusion and cell viability in the Dox-treated cardiomyocytes (Fig. 4A-E). Meanwhile, Pae's inhibitory effects on mitochondrial oxidative stress (Fig. 4B and F), apoptosis (Fig. 4G and H) and LDH release (Fig. 4I) were blunted in the Dox-treated cardiomyocvtes when Mfn2 was knocked down. Cardiac-specific Mfn2 knockout mice (Mfn2<sup>-/-</sup>) were generated by crossing the mice homozygous for the floxed Mfn2 alleles (Mfn2<sup>fl/fl</sup>) with Myh6-Mer-Cre-Mer (tamoxifen-inducible heart-specific Cre) mice (Supplementary Fig. S4A). Mfn2 protein expression was specifically absent in cardiac tissues of Mfn2<sup>-/-</sup> mice (Supplementary Fig. S4B). Pae administration restored the decreased expression of Mfn2, alleviated cardiac dysfunction, inhibited oxidative stress

and reduced myocardial apoptosis in the Dox-treated Mfn2<sup>fl/fl</sup> mice but not in Mfn2<sup>-/-</sup> mice (Supplementary Fig. S5A-G). Moreover, Pae administration enhanced the activity of complexes I, III in the Dox-treated Mfn2<sup>fl/fl</sup> mice but not in Mfn2<sup>-/-</sup> mice (Supplementary Fig. S5H). These findings suggested that Pae provided mitochondrial and cardiac protection in the Dox-treated hearts via an Mfn2-dependent way.

Pae increased Mfn2 expression via Stat3-mediated transcription

To further elucidate the signaling mechanism that mediates the upregulation effect of Pae on Mfn2, several specific inhibitors were used to block the potential signaling pathway. The most common pathways related to cardioprotection include MEK/ERK, PI3K/Akt, JAK, Stat3 and PKC signaling [36,37]. Thus, we choose to use the inhibitors of these signaling pathways based on their cardioprotective characteristics. The following inhibitors were used to incubate the cardiomyocytes in the Dox + Pae group: PD98059 (a MEK/ERK inhibitor, 10 µM; MedChem Express) [38]; Wortmannin (a PI3K/ Akt inhibitor, 0.1 μM; MedChem Express) [38,39]; Ruxolitinib (Ruxo, a JAK inhibitor, 1 μM; MedChem Express) [40,41]; Stattic (a Stat3 inhibitor, 10 uM; MedChem Express) [42] and Bisindolylmaleimide XI hydrochloride (Bis XI, a PKC inhibitor targeting isoform  $\alpha$ ,  $\beta$ ,  $\gamma$ ,  $\epsilon$ , 2  $\mu$ M; MedChem Express) [43]. Pretreatment with Bis XI or Stattic largely blunted Pae-induced elevation of Mfn2 in Dox-treated cardiomyocytes, while Pae-induced elevation of Mfn2 was unaffected by Wortmannin, PD98059, or Ruxo (Fig. 5A). Pretreatment with bisindolylmaleimide I (Bis I, a PKC inhibitor targeting isoform  $\alpha$ ,  $\beta$ ,  $\gamma$ , 10  $\mu$ M [44], MedChem Express) had no significant effect on Pae-induced elevation of Mfn2 (Supple-

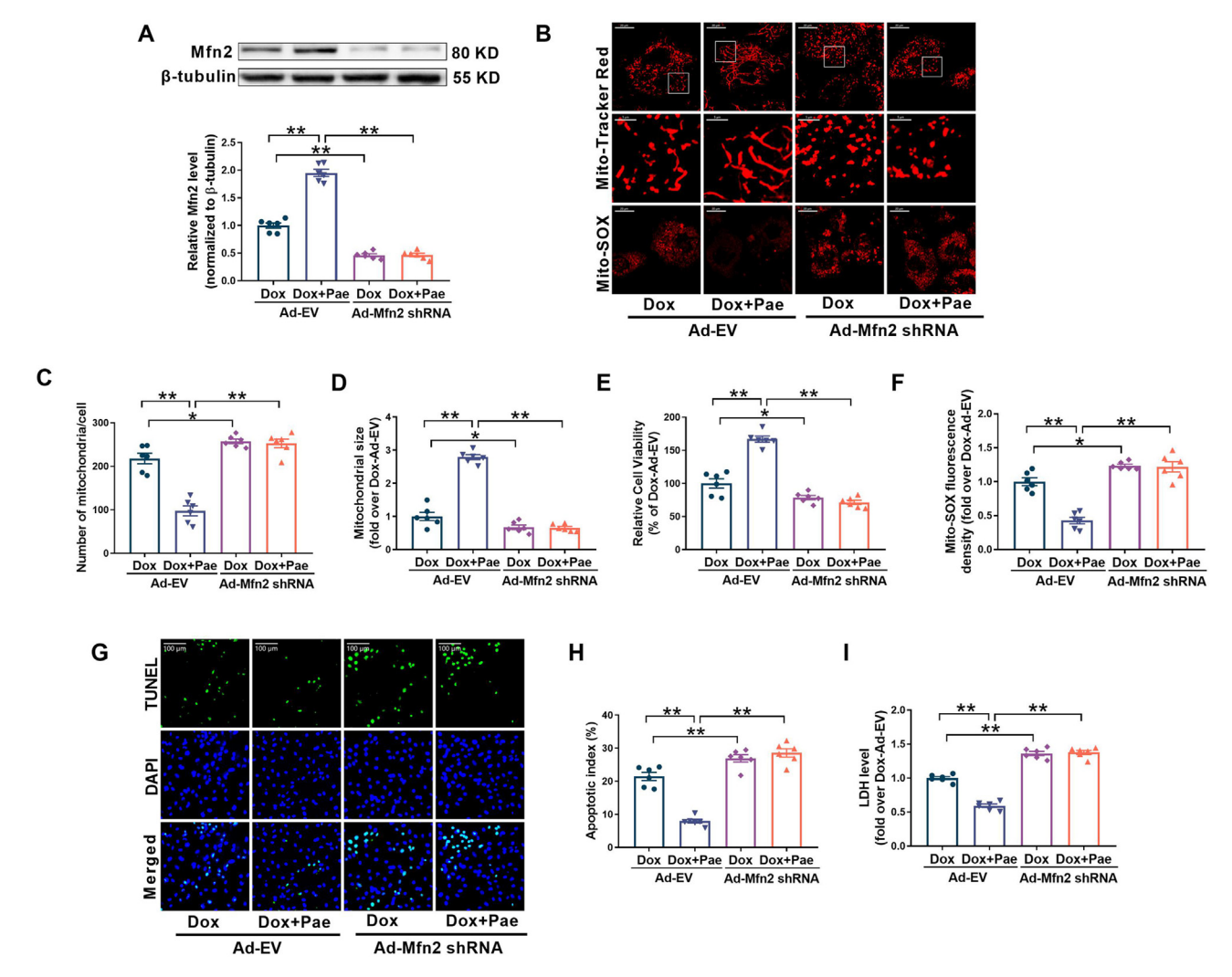


Fig. 4. Knockdown of Mfn2 blunted the protective properties of Pae against Dox-induced mitochondrial and cellular injury. (A) Representative blots and quantitative data of Mfn2 expression. (B) Representative images of MitoTracker Red-stained mitochondrial morphology (upper, quantitative data are presented in C-D) and mitochondrial derived superoxide production stained with MitoSOX (bottom, quantitative data are presented in F). Original magnification  $\times$  600. (C) Quantitative data of mitochondrial number per cell. (D) Quantitative data of mean mitochondrial size. (E) Relative cell viability. (F) Quantitative data of relative mitochondrial ROS fluorescence density. (G) Representative images of TUNEL and DAPI staining. Original magnification  $\times$  200. (H) Quantitative data of the apoptotic index. (I) Lactate dehydrogenase (LDH) release determined in cell supernatant. n = 6 per group. \*P < 0.05, \*\*P < 0.01. (For interpretation of the references to colour in this figure legend, the reader is referred to the web version of this article.)

mentary Fig S6A). Mfn2 expression was unaffected by these inhibitors in the Dox-treated cardiomyocytes without Pae (Supplementary Fig S6B). Since the distinguishing feature between Bis I and Bis XI is that PKC $\epsilon$  isoform could be inhibited by Bis XI but not Bis I, these results indicated that Pae-induced elevation of Mfn2 may require the activation of PKC $\epsilon$ .  $\epsilon$ V1-2 (a PKC $\epsilon$  inhibitor peptide) or Stattic (a Stat3 inhibitor) was further utilized to investigate the relationship between PKC $\epsilon$  and Stat3 involved in the effects of Pae. It was shown that the upregulation of Pae on phosphorylated Stat3 at Tyr705 (the active form of Stat3) was inhibited by  $\epsilon$ V1-2, whereas Stattic did not affect the upregulating effects of Pae on PKC $\epsilon$ , indicating that PKC $\epsilon$  was the upstream of Stat3 in the pathway activated by Pae (Supplementary Fig. S6C-F).

Stat3 was knocked down using siRNA to see whether it was essential for regulating Mfn2-mediated mitochondrial fusion. As indicated in Fig. 5, Stat3 knockdown lowered Stat3 phosphorylation (Fig. 5B) and inhibited Mfn2-mediated mitochondrial fusion (Fig. 5B-I) and cell viability (Fig. 5J) in the Dox-treated cardiomyocytes. Subsequently, Stat3 siRNA augmented mitochondrial oxidative stress (Fig. 5K) and increased cardiomyocyte apoptosis

as well as LDH release under Dox conditions. Moreover, knockdown of Stat3 not only blocked Pae's promoting effects on Mfn2-mediated mitochondrial fusion (Fig. 5B-I) and cell viability (Fig. 5J), but also blunted Pae's inhibition on mitochondrial oxidative stress (Fig. 5K), apoptosis (Fig. 5L and M) and LDH release (Fig. 5N) in the Dox-treated cardiomyocytes. Stat3 was found to be directly bound to the promoter of Mfn2 using chromatin immunoprecipitation (ChIP)-PCR. Treatment with Dox decreased the binding of Stat3 to the Mfn2 promoter, which was rescued by Pae treatment (Fig. 5O). These data indicated that Stat3 was directly involved in Pae's promoting effects on Mfn2-mediated mitochondrial fusion.

Pae activated Stat3-Mfn2 signaling pathway via upregulating PKCε

Since Pae is a liposoluble compound with a low molecular weight that is easily transported to the brain [45], we supposed that Pae may be able to pass across cell membranes and directly interact with some adaptor molecules. The PKCE C2 domain is a vital player in PKCE activation [46]. We try to use computation

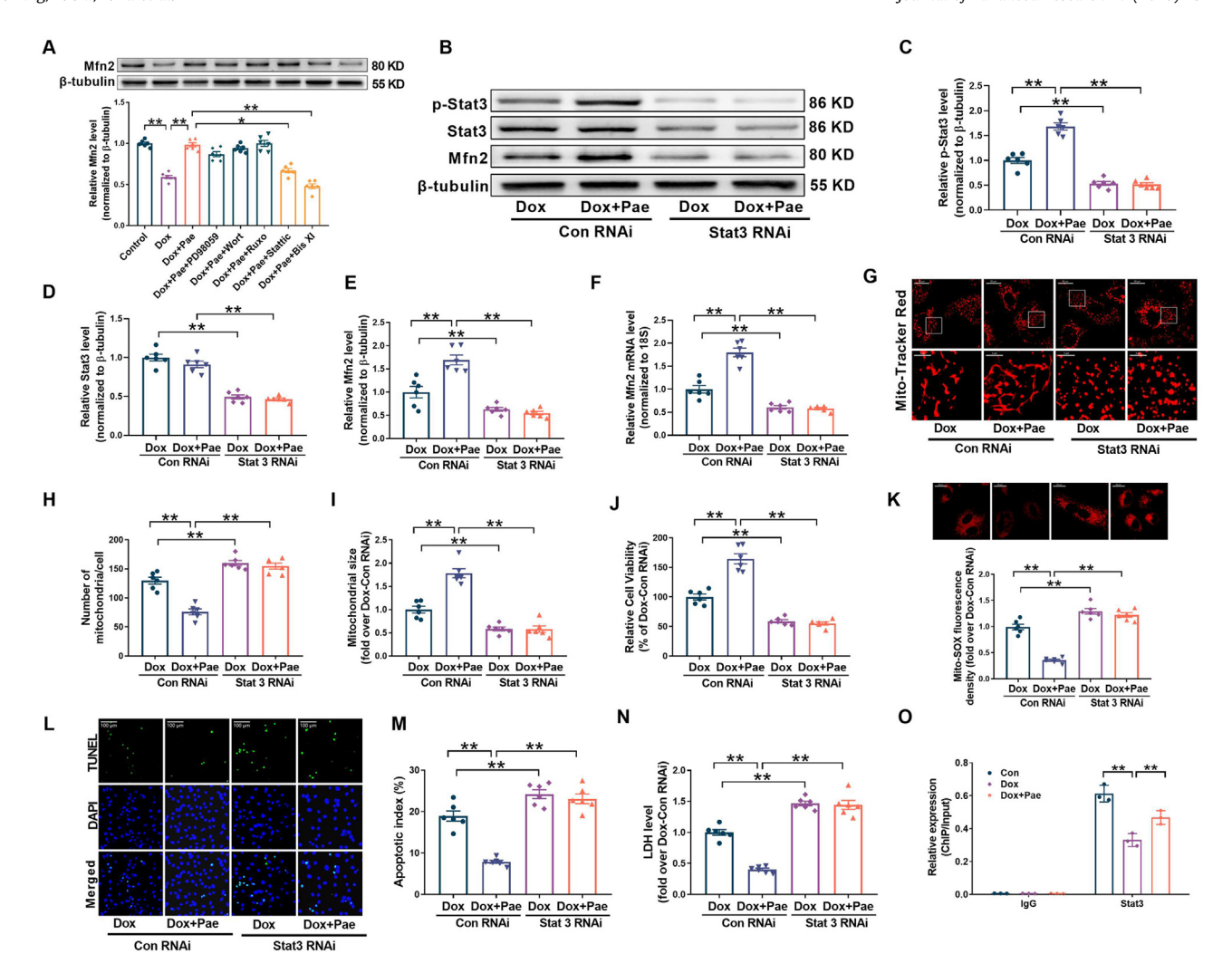
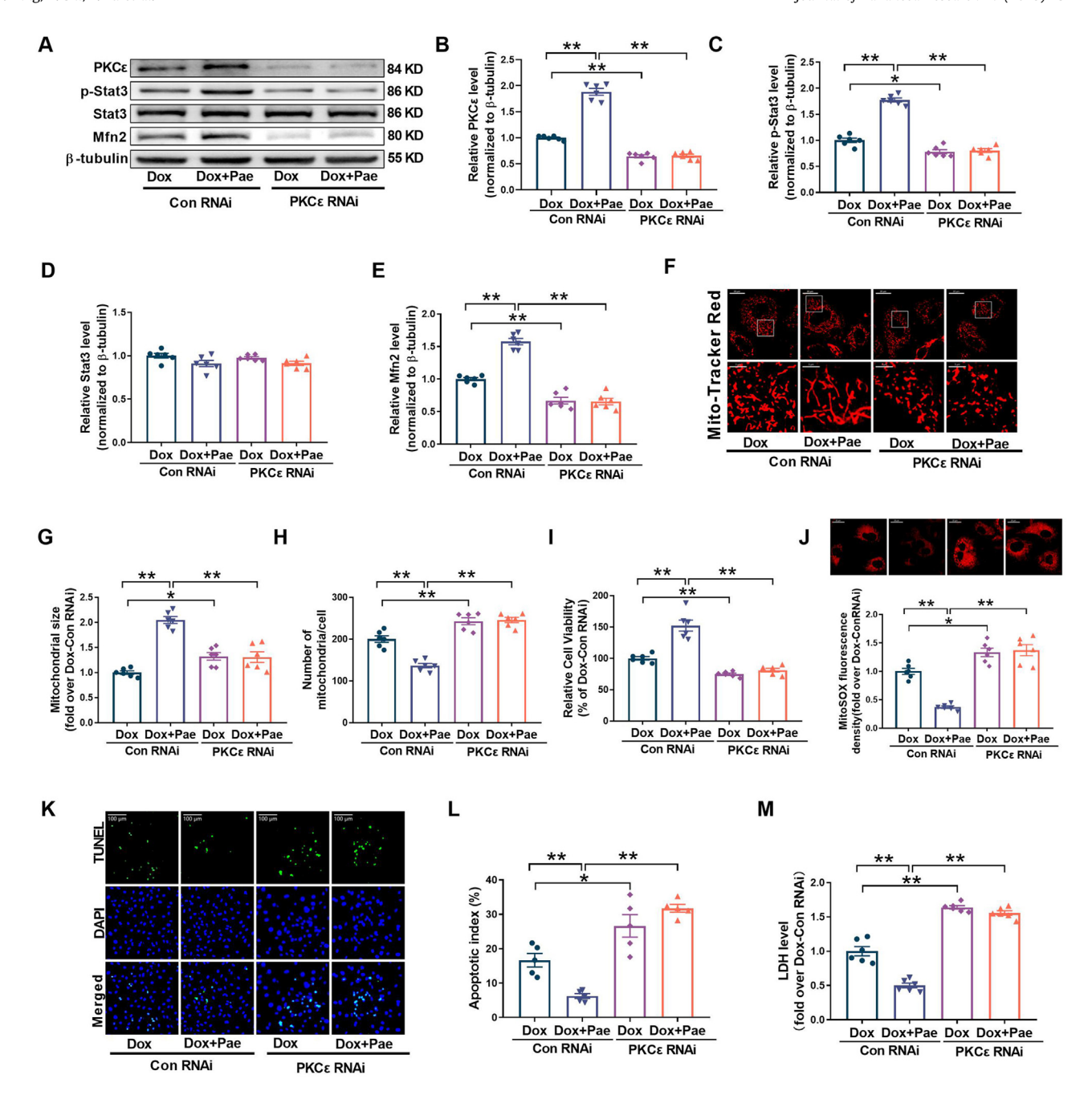


Fig. 5. Pae elevated Mfn2 expression via Stat3-mediated transcription. (A) Representative blots and quantitative data of Mfn2. (B-E) Representative blots and quantitative data of phosphorylated Stat3 (p-Stat3), total Stat3 and Mfn2. (F) Quantitative data of Mfn2 mRNA expression. (G) MitoTracker Red-stained mitochondrial morphology images. Original magnification × 600. (H) Quantitative data of mitochondrial number per cell. (I) Quantitative data of mean mitochondrial size. (J) Relative cell viability. (K) Representative images and quantitative data of MitoSOX-stained mitochondrial ROS. (L) Representative images of TUNEL and DAPI staining. Original magnification × 200. (M) Quantitative data of the apoptotic index. (N) Lactate dehydrogenase (LDH) release determined in cell supernatant. (O) Chromatin immunoprecipitation (ChIP) analysis of Stat3 at the position of Mfn2 promoter. n = 6 per group. \*\*P < 0.01. (For interpretation of the references to colour in this figure legend, the reader is referred to the web version of this article.)

docking to investigate the interaction between Pae and PKCE C2 domain. Supplementary Fig. S7A illustrated the 2D and 3D structures of Pae. Computation docking found that the maximum binding affinity between Pae and the PKCε C2 domain was predicted to be -4.1 kcal/mol, which suggested that Pae may bind to PKCE (Supplementary Fig. S7B). The physical binding of Pae to PKC was further detected using the SPR-based Biacore assay. The data of response units, a parameter used to assess Pae's binding to the PKCε protein, showed a dose-dependent pattern. The equilibrium dissociation constant (KD) was calculated to be around 38.25 mol/L, indicating a relatively high affinity between Pae and PKCE (Supplementary Fig. S7C). Meanwhile, Dox dosedependently bound to PKCE protein with an equilibrium dissociation constant (KD) value of 44.79 µmol/L (Supplementary Fig. S7D). The cellular experiment revealed that Dox-induced reduction of PKC expression and activity was restored by Pae (Supplementary Fig. S7E and S7F). Nevertheless, Dox or Pae did not significantly change the pre-mRNA and mRNA levels of PKCE (Supplementary Fig. S7G and S7H). Treatment with the proteasome inhibitor MG132 (10  $\mu M$ , 30 min prior to Dox) significantly restored the protein expression of PKCE in the Dox-treated cardiomyocytes (Supplementary Fig. S7I). Pae did not further increase the expression of PKCɛ under the Dox conditions following treatment with MG132 (Supplementary Fig. S7I). These results suggest that PKCɛ expression may be regulated via the proteasome pathway. Co-immunoprecipitation experiments indicated that Stat3 was precipitated with PKCɛ antibody (Supplementary Fig. S7J), suggesting that PKCɛ may interact with Stat3 directly and induce Stat3 activation through phosphorylation.

PKCE siRNA was further used to determine whether PKCE was responsible for Pae-induced promotion of Stat3 phosphorylation and Mfn2-mediated mitochondrial fusion. It was shown that knockdown of PKCE reduced the phosphorylation of Stat3 (Fig. 6-A-D) and inhibited Mfn2-mediated mitochondrial fusion (Fig. 6E-H) as well as cell viability (Fig. 6I) in the Dox-treated cardiomyocytes. Subsequently, PKCE siRNA augmented mitochondrial oxidative stress (Fig. 6J) and increased cardiomyocyte apoptosis as well as LDH release (Fig. 6K-M) under the Dox conditions. Importantly, knockdown of PKCE not only diminished Pae-induced activation in Stat3-Mfn2 signaling pathway and promotion of mitochondrial fusion (Fig. 6A-H) and cell viability (Fig. 6I), but also blunted Pae-induced inhibition in mitochondrial oxidative stress (Fig. 6J) and cardiomyocyte apoptosis (Fig. 6K and L) as well as LDH release (Fig. 6M) in the Dox-treated cardiomyocytes. The



**Fig. 6. Knockdown of PKC**εdiminished **Pae-induced activation in Stat3-Mfn2 signaling pathway. (A-E)** Representative blots and quantitative data of PKCε, phosphorylated Stat3 (p-Stat3), total Stat3 and Mfn2. **(F)** Representative MitoTracker Red-stained mitochondrial morphology images. Original magnification  $\times$  600. **(G)** Quantitative data of mean mitochondrial size. **(H)** Quantitative data of mitochondrial number per cell. **(I)** Relative cell viability. **(J)** Representative images and quantitative data of MitoSOX-stained mitochondrial ROS. **(K)** Representative images of TUNEL and DAPI staining. Original magnification  $\times$  200. **(L)** Quantitative data of the apoptotic index. **(M)** Lactate dehydrogenase (LDH) release determined in cell supernatant. n = 6 per group. \*P < 0.05, \*\*P < 0.01. (For interpretation of the references to colour in this figure legend, the reader is referred to the web version of this article.)

enhancing effects of Pae on PKC $\epsilon$  expression and Stat3 phosphorylation were verified *in vivo* in the Dox-treated hearts (Supplementary Fig. S8A-D). These findings indicated that PKC $\epsilon$  might act as a phytochemical ligand of Pae to activate Stat3-Mfn2 signaling pathway and promote mitochondrial fusion.

Pae did not interfered with the antitumor activity of Dox

Finally, to assess the prospective use of Pae as a cardioprotective medicine in the setting of Dox treatment, we explored whether the antitumor effect of Dox was affected by Pae. CCK8 assay was used to determine the survival curve of B16 cells exposed to vari-

ous concentrations of Dox (0.3, 1, 3  $\mu$ mol/L) for 24 h with or without Pae (50  $\mu$ mol/L). As shown in Supplementary Fig. S9A, Dox or Pae alone could inhibit cell viability in the Dox-sensitive B16 tumor cells. The effect of Dox was dose-dependent. Pae enhanced the inhibitory effects of low-concentration Dox (0.3 and 1  $\mu$ M) on cell viability, although it did not affect the action of high-concentration Dox (3  $\mu$ M). Tumor-bearing mice were constructed to further validate the combined effects of Dox and Pae *in vivo* (Supplementary Fig. S9B). Dox also exerted a dose-dependent antitumor effect on B16 melanoma in tumor-bearing mice. Pae not only attenuated tumor growth alone but also further delayed tumor growth in the presence of low-dose Dox (5 mg/kg), resulting

in considerably smaller tumors in Dox (5 mg/kg) + Pae group than in Dox (5 mg/kg) group (Supplementary Fig. S9B-C). Dox-induced myocardial injury (serum cTnT levels) was reduced at the low dose (5 mg/kg) compared with the high dose (15 mg/kg). Pae further reduced myocardial injury induced by low-dose Dox (Supplementary Fig. S9D). These data indicated that Pae may help to reduce the dose of Dox and alleviate myocardial injury in Dox-based chemotherapy against B16 melanoma. Moreover, the effects of Pae on Dox's anticancer action was explored in some other models of Dox-sensitive tumors including SNU-368 (human Hepatocarcinoma Cells), Hepa 1–6 (Mouse Hepatocarcinoma Cells) and 4 T1 (Mouse Breast Carcinoma Cells). As shown in Supplementary Fig. S10, Pae did not enhance the inhibitory effects of Dox in these tumor cells. These results demonstrated that Pae did not interfere with the anti-tumor efficacy of Dox in some other tumors.

## Discussion

Pae has been proven to offer therapeutic promise for a range of diseases, including osteoarthritis, rheumatoid arthritis, cardiovascular diseases and cancer [47]. Its wide therapeutic benefits are due to a variety of biological activities such as anti-cytokine, anti-inflammatory, and anti-oxidative actions [47]. In the cardiovascular system, recent reports show that Pae attenuates transverse aortic constriction-induced cardiac dysfunction through ERK1/2 signaling [48] and reduces cytotoxic drug-induced myocardial injury via PI3K/Akt signaling [49]. Dox accumulates predominantly in nuclei and mitochondria, with the latter accounting for Dox's cardio-selective toxicity [11,50]. Few research has explored Pae's beneficial effects on mitochondria, especially under the Dox conditions. Our study was the first to present that Pae improves mitochondrial function and cardiac performance via promoting Mfn2-mediated mitochondrial fusion in the Dox-treated hearts. Moreover, the promoting effect of Pae is mediated through Stat3 but not ERK1/2 or PI3K/Akt signaling that has been reported previously. Mechanistically, Pae binds to and upregulates PKCE, which then interacts with Stat3 and facilitates the phosphorylation and activation of the Stat3 that binds to the Mfn2 promoter to enhance mitochondrial fusion (Supplementary Fig. S11). To summarize, our study identifies Pae as a prospective therapeutic drug against Doxinduced cardiac injury while maintaining Dox's anticancer activity.

Mitochondrial dysfunction is characterized by increased ROS production that is the primary mechanism through which Dox causes myocardial damage [51,52]. Previous research has linked mitochondrial fusion with lower mitochondrial ROS generation and apoptosis [53]. Therefore, promoting mitochondrial fusion might be a useful therapeutic strategy for preventing Doxinduced cardiac injury. In this study, a medium dose of Pae (150 mg/kg/d) was found to be the most effective for protective effects in the rats. Pae concentrations in plasma were shown to be about 1 µg/ml (6 µmol/L) after the rats were given 20 mg/kg Pae orally [54]. Therefore, after oral administration of Pae at 150 mg/kg, the blood concentration approximately reached 45 μmol/L. Interestingly, this concentration is consistent with the most effective concentration (50 µmol/L) in our cellular study, suggesting that a moderate dose or concentration of Pae may produce the best therapeutic effects against Dox-induced cardiotoxicity.

Mitochondrial fusion is regulated by Mfn1/Mfn2 localized in the mitochondrial outer membrane, and Opa1 localized in the mitochondrial inner membrane [55]. Previous studies have reported that the level of fusion-related proteins Mfn1, Mfn2 and Opa1 proteins were lower after seven weeks of continuous Dox injections in rats [56]. In this research, we noticed that only Mfn2 expression was reduced in Dox-treated hearts after three weeks of continuous Dox injections, while other mitochondrial fusion proteins, such as

Mfn1 and Opa1, exhibited no significant change in expression. It seems that the downregulation of Mfn2 is an early change upon Dox insult. How Dox suppressed Mfn2-mediated mitochondrial fusion in the hearts have not been well understood. One novelty of our research is that we have found that the downregulated PKCɛ-Stat3 signaling pathway is responsible for the lower transcriptional expression of Mfn2 as well as the inhibition of mitochondrial fusion in Dox-treated hearts.

Stat3 is a transcription factor that is activated when it is phosphorylated at Tyr705, leading to its translocation from the cytoplasm to the nucleus to induce specific gene expression [57]. Zhao et al. have demonstrated that the expression of p-Stat3 Tyr705 was significantly reduced after Dox treatment in mice and in Dox-induced H9c2 cardiomyocytes in vitro [58]. This downregulation of phosphorylated Stat3 level was also observed in Doxinduced neonatal rat cardiomyocytes [59.60] These findings indicated that decreased cardiac Stat3 phosphorylation and activation are common features in Dox-induced myocardial injury models. Consistent with the previous reports, we also found that Stat3 phosphorylation at Tyr705 was reduced in both Dox-treated hearts and cardiomyocytes. Furthermore, our study found that Dox repressed the binding of Stat3 to Mfn2 promoter and the binding was largely recovered after Pae therapy. This qualitative study sheds light on the detailed downstream mechanisms by which Pae enhances Mfn2-mediated mitochondrial fusion.

Despite the fact that Dox has been shown to have cardiotoxic effects [24,25,61], the direct molecular target of Dox remains unclear. We are the first to show that Dox has the ability to bind to and downregulate PKCE, while the binding of Pae to PKCE restores the PKCE-Stat3-Mfn2 signaling pathway. PKCE is a protein kinase that has anti-inflammatory properties [62] and cardiac protection [63,64]. Xiong et al. have found that norepinephrine-induced ROS production significantly reduces PKCE transcription activity and protein expression *in vitro* and *in vivo* [65]. In our study, proteasome pathway plays a key role in the decrease of PKCE expression caused by Dox. The binding of Pae to PKCE may help PKCE resist proteasomal degration and restore its expression and activity.

In addition, Pae has been demonstrated to act as an anti-tumor agent. Ou's study has found that Pae has the inhibitory effects on tumor cell growth in mice bearing breast carcinoma [66]. Although previous studies have reported the antitumor action of Pae alone in several tumor models such as gastric cancer [67] and liver cancer [68], the effects of Pae on Dox's antitumor activity remain largely unclear. We have revealed that Pae increases the antitumor activity of low-dose Dox in the B16 melanoma and does not interfere with Dox's antitumor efficacy in some other tumor cells, suggesting Pae could be used in combination with Dox during the process of chemotherapy. Moreover, Pae further reduced myocardial injury even under the condition of low-dose Dox, which make the myocardium nearly free of injury. This work indicates that Pae is an ideal therapeutic agent during Dox-based chemotherapy treatment.

Notably, our study still has several limitations. First, the PKCɛ-Stat3-Mfn2 signaling pathway may not be the only pathway by which Pae exerts the protective effect on mitochondrial. It is also possible that Pae acts in other signaling pathways, which needs further investigation. Second, we explored the role of PKCɛ-Stat3 signaling in the protective effects of Pae primarily at the cellular level using PKCɛ or Stat3 inhibitor/siRNA, and the use of cardiac-specific PKCɛ or Stat3 knockout animals will be very useful in further elucidating the role of PKCɛ-Stat3 in Mfn2-mediated mitochondrial fusion. Third, the impacts of Pae on Dox's antitumor efficacy were mainly investigated in several tumor cells. Given the variability and complexity of tumors, assessing the impact of Pae in all Dox-sensitive tumor models is difficult. Since Pae is

widely regarded as a possible tumor suppressor drug [47], we assume that Pae at least does not interfere with Dox's anticancer efficacy. Despite these limitations, we consider that our findings have revealed potential therapeutic strategies for Dox-induced cardiotoxicity.

#### Conclusion

In conclusion, our findings demonstrate that Pae defends against Dox-induced myocardial injury via activating the PKC&Stat3-Mfn2 pathway without interfering with Dox's anticancer properties. It is proved that Pae binds to and upregulates PKC& to increase Stat3 phosphorylation, which subsequently binds to the Mfn2 promoter to enhance Mfn2-mediated mitochondrial fusion. These findings may favor Pae as a promising new therapeutic medication candidate for preventing Dox-induced cardiotoxicity in the clinic.

## **Funding**

This study was supported by the grants from National Natural Science Foundation of China (No. 81970316, No. 82070387, No. 82111530058), Key Research and Development Plan of Shaanxi (No. 2021SF-141, 2022KWZ-18).

## Compliance with Ethics Requirements.

All experiments involving animals were conducted according to the ethical policies and procedures approved by the ethics committee of the Xi'an Jiaotong University (Approval no. 2019–505, Xi'an, Shaanxi, China). All the studies in our experiments are conducted in compliance with the National Institutes of Health Guidelines for Use of Laboratory Animals (8th Edition, 2011). Extensive efforts were made to ensure minimal suffering of the animals used during the study.

## **CRediT authorship contribution statement**

Mingge Ding: Writing – original draft. Rui Shi: Animal experiments, cellular experiments and molecular biology experiments. Data analysis. Feng Fu: Animal experiments, cellular experiments and molecular biology experiments. Man Li: Cellular experiments and molecular biology experiments. Dema De: Molecular biology experiments. Yanyan Du: Molecular biology experiments. Zongfang Li: Conceptualization, Supervision, Writing – review & editing.

## **Declaration of Competing Interest**

The authors declare that they have no known competing financial interests or personal relationships that could have appeared to influence the work reported in this paper.

## Appendix A. Supplementary material

Supplementary data to this article can be found online at https://doi.org/10.1016/j.jare.2022.07.002.

# References

- [1] Chuang E, Wiener N, Christos P, Kessler R, Cobham M, Donovan D, et al. Phase I trial of ixabepilone plus pegylated liposomal doxorubicin in patients with adenocarcinoma of breast or ovary. Ann Oncol 2010;21(10):2075–80.
- [2] Dhir AA, Sawant SP. Cardiac morbidity & mortality in patients with breast cancer: a review. Indian J Med Res 2021;154:199–209. doi: <a href="https://doi.org/10.4103/jimr.IJMR-879-20">https://doi.org/10.4103/jimr.IJMR-879-20</a>.

- [3] Lipshultz SE, Miller TL, Scully RE, Lipsitz SR, Rifai N, Silverman LB, et al. Changes in cardiac biomarkers during doxorubicin treatment of pediatric patients with high-risk acute lymphoblastic leukemia: associations with long-term echocardiographic outcomes. J Clin Oncol 2012;30(10):1042–9.
- [4] Omland T, Heck SL, Gulati G. The role of cardioprotection in cancer therapy cardiotoxicity: JACC: cardiooncology state-of-the-art review. JACC CardioOncol 2022;4:19–37. doi: <a href="https://doi.org/10.1016/j.jaccao.2022.01.101">https://doi.org/10.1016/j.jaccao.2022.01.101</a>.
- [5] Seifert CF, Nesser ME, Thompson DF. Dexrazoxane in the prevention of doxorubicin-induced cardiotoxicity. Ann Pharmacother 1994;28:1063–72. doi: https://doi.org/10.1177/106002809402800912.
- [6] Tebbi CK, London WB, Friedman D, Villaluna D, De Alarcon PA, Constine LS, et al. Dexrazoxane-associated risk for acute myeloid leukemia/myelodysplastic syndrome and other secondary malignancies in pediatric hodgkin's disease. J Clin Oncol 2007;25(5):493–500.
- [7] Vuong JT, Stein-Merlob AF, Cheng RK, Yang EH. Novel therapeutics for anthracycline induced cardiotoxicity. Front Cardiovasc Med 2022;9:. doi: https://doi.org/10.3389/fcvm.2022.863314863314.
- [8] Marin-Garcia J, Akhmedov AT. Mitochondrial dynamics and cell death in heart failure. Heart Fail Rev 2016;21:123–36. doi: <a href="https://doi.org/10.1007/s10741-016-9530-2">https://doi.org/10.1007/s10741-016-9530-2</a>.
- [9] Khuanjing T, Ongnok B, Maneechote C, Siri-Angkul N, Prathumsap N, Arinno A, et al. Acetylcholinesterase inhibitor ameliorates doxorubicin-induced cardiotoxicity through reducing rip1-mediated necroptosis. Pharmacol Res 2021;173:105882.
- [10] Scicchitano M, Carresi C, Nucera S, Ruga S, Maiuolo J, Macrì R, et al. Icariin protects H9C2 rat cardiomyoblasts from doxorubicin-induced cardiotoxicity: role of caveolin-1 upregulation and enhanced autophagic response. Nutrients 2021;13(11):4070.
- [11] Wallace KB, Sardao VA, Oliveira PJ. Mitochondrial determinants of doxorubicin-induced cardiomyopathy. Circ Res 2020;126:926–41. doi: https://doi.org/10.1161/CIRCRESAHA.119.314681.
- [12] Marin-Garcia J, Akhmedov AT, Moe GW. Mitochondria in heart failure: the emerging role of mitochondrial dynamics. Heart Fail Rev 2013;18:439–56. doi: https://doi.org/10.1007/s10741-012-9330-2.
- [13] Wu C, Zhang Z, Zhang W, Liu X. Mitochondrial dysfunction and mitochondrial therapies in heart failure. Pharmacol Res 2022;175:. doi: <a href="https://doi.org/10.1016/j.phrs.2021.106038">https://doi.org/10.1016/j.phrs.2021.106038</a>106038.
- [14] Forte M, Schirone L, Ameri P, Basso C, Catalucci D, Modica J, et al. The role of mitochondrial dynamics in cardiovascular diseases. Br J Pharmacol 2021;178 (10):2060–76.
- [15] Osataphan N, Phrommintikul A, Chattipakorn SC, Chattipakorn N. Effects of doxorubicin-induced cardiotoxicity on cardiac mitochondrial dynamics and mitochondrial function: Insights for future interventions. J Cell Mol Med 2020;24:6534–57. doi: <a href="https://doi.org/10.1111/jcmm.15305">https://doi.org/10.1111/jcmm.15305</a>.
- [16] Qin Y, Li A, Liu B, Jiang W, Gao M, Tian X, et al. Mitochondrial fusion mediated by fusion promotion and fission inhibition directs adult mouse heart function toward a different direction. FASEB | 2020;34(1):663–75.
- [17] Tong M, Zablocki D, Sadoshima J. The role of Drp1 in mitophagy and cell death in the heart. J Mol Cell Cardiol 2020;142:138–45. doi: <a href="https://doi.org/10.1016/j.vimcc.2020.04.015">https://doi.org/10.1016/j.vimcc.2020.04.015</a>.
- [18] Li H, Song F, Duan L-R, Sheng J-J, Xie Y-H, Yang Q, et al. Paeonol and danshensu combination attenuates apoptosis in myocardial infarcted rats by inhibiting oxidative stress: roles of Nrf2/HO-1 and Pl3K/Akt pathway. Sci Rep 2016;6(1). doi: https://doi.org/10.1038/srep23693.
- [19] Tsai C-F, Su H-H, Chen K-M, Liao J-M, Yao Y-T, Chen Y-H, et al. Paeonol protects against myocardial ischemia/reperfusion-induced injury by mediating apoptosis and autophagy crosstalk. Front Pharmacol 2021;11:. doi: <a href="https://doi.org/10.3389/fphar.2020.586498">https://doi.org/10.3389/fphar.2020.586498</a>586498.
- [20] Wang X, Zhu G, Yang S, Wang X, Cheng H, Wang F, et al. Paeonol prevents excitotoxicity in rat pheochromocytoma PC12 cells via downregulation of ERK activation and inhibition of apoptosis. Planta Med 2011;77(15):1695–701.
- [21] Liu C, Han Y, Gu X, Li M, Du Y, Feng N, et al. Paeonol promotes Opa1-mediated mitochondrial fusion via activating the CK2alpha-Stat3 pathway in diabetic cardiomyopathy. Redox Biol 2021;46:. doi: <a href="https://doi.org/10.1016/ji.redox.2021.102098">https://doi.org/10.1016/ji.redox.2021.102098</a> 102098.
- [22] Wang P, Wang L, Lu J, Hu Y, Wang Q, Li Z, et al. Sesn2 protects against doxorubicin-induced cardiomyopathy via rescuing mitophagy and improving mitochondrial function. J Mol Cell Cardiol 2019;133:125–37.
- [23] Zhou L, Li R, Liu C, Sun T, Htet Aung LH, Chen C, et al. Foxo3a inhibits mitochondrial fission and protects against doxorubicin-induced cardiotoxicity by suppressing MIEF2. Free Radic Biol Med 2017;104:360–70.
- [24] Xia Y, Chen Z, Chen Ao, Fu M, Dong Z, Hu K, et al. LCZ696 improves cardiac function via alleviating Drp1-mediated mitochondrial dysfunction in mice with doxorubicin-induced dilated cardiomyopathy. J Mol Cell Cardiol 2017;108:138-48.
- [25] Lu J, Li J, Hu Y, Guo Z, Sun D, Wang P, et al. Chrysophanol protects against doxorubicin-induced cardiotoxicity by suppressing cellular parylation. Acta Pharm Sin B 2019:9(4):782–93.
- [26] Ma L, Chuang CC, Weng W, Zhao L, Zheng Y, Zhang J, et al. Paeonol protects rat heart by improving regional blood perfusion during no-reflow. Front Physiol 2016;7:298. doi: <a href="https://doi.org/10.3389/fphys.2016.00298">https://doi.org/10.3389/fphys.2016.00298</a>.
- [27] Zhang L, Ma C, Gu R, Zhang M, Wang X, Yang L, et al. Paeonol regulates hypoxia-induced proliferation of pulmonary artery smooth muscle cells via EKR 1/2 signalling. Eur J Pharmacol 2018;834:257–65.
- [28] Jin L, Huang R, Huang X, Zhang B, Ji M, Wang H. Discovery of 18βglycyrrhetinic acid conjugated aminobenzothiazole derivatives as Hsp90-

- Cdc37 interaction disruptors that inhibit cell migration and reverse drug resistance. Bioorg Med Chem 2018;26:1759–75. doi: https://doi.org/10.1016/j.bmc.2018.02.021.
- [29] Li Z, Wu X, Jia L, Li J, Zhang R, Tang H, et al. Design and synthesis of novel 2-arylbenzimidazoles as selective mutant isocitrate dehydrogenase 2 r140q inhibitors. Bioorg Med Chem Lett 2020;30(9):127070.
- [30] Nie X, Tang W, Zhang Z, Yang C, Qian L, Xie X, et al. Procyanidin b2 mitigates endothelial endoplasmic reticulum stress through a PPARdelta-dependent mechanism. Redox Biol 2020;37:. doi: <a href="https://doi.org/10.1016/ji.redox.2020.101728">https://doi.org/10.1016/ji.redox.2020.101728</a>101728.
- [31] Jamal J, Mustafa MR, Wong PF. Paeonol protects against premature senescence in endothelial cells by modulating Sirtuin 1 pathway. J Ethnopharmacol 2014;154:428–36. doi: <a href="https://doi.org/10.1016/j.jep.2014.04.025">https://doi.org/10.1016/j.jep.2014.04.025</a>.
- [32] Zhao X, Fang J, Li S, Gaur U, Xing X, Wang H, et al. Artemisinin attenuated hydrogen peroxide (H<sub>2</sub>O<sub>2</sub>)-induced oxidative injury in SH-SY5Y and hippocampal neurons via the activation of AMPK pathway. Int J Mol Sci 2019;20(11):2680.
- [33] Mousa HSE, Abdel Aal SM, Abbas NAT. Umbilical cord blood-mesenchymal stem cells and carvedilol reduce doxorubicin-induced cardiotoxicity: possible role of insulin-like growth factor-1. Biomed Pharmacother 2018;105:1192-204. doi: https://doi.org/10.1016/j.biopha.2018.06.051.
  [34] Zhang Y, Ahmad KA, Khan FU, Yan S, Ihsan AU, Ding Q. Chitosan
- [34] Zhang Y, Ahmad KA, Khan FU, Yan S, Ihsan AU, Ding Q. Chitosan oligosaccharides prevent doxorubicin-induced oxidative stress and cardiac apoptosis through activating p38 and JNK MAPK mediated Nrf2/ARE pathway. Chem Biol Interact 2019;305:54–65. doi: <a href="https://doi.org/10.1016/j.cbi.2019.03.027">https://doi.org/10.1016/j.cbi.2019.03.027</a>.
- [35] Boengler K, Kosiol M, Mayr M, Schulz R, Rohrbach S. Mitochondria and ageing: role in heart, skeletal muscle and adipose tissue. J Cachexia Sarcopenia Muscle 2017;8:349–69. doi: https://doi.org/10.1002/icsm.12178.
- [36] Boengler K, Hilfiker-Kleiner D, Drexler H, Heusch G, Schulz R. The myocardial JAK/STAT pathway: from protection to failure. Pharmacol Ther 2008;120:172–85. doi: https://doi.org/10.1016/j.pharmthera.2008.08.002.
- [37] Downey JM, Davis AM, Cohen MV. Signaling pathways in ischemic preconditioning. Heart Fail Rev 2007;12:181–8. doi: <a href="https://doi.org/10.1007/s10741-007-9025-2">https://doi.org/10.1007/s10741-007-9025-2</a>
- [38] He SF, Jin SY, Wu H, Wang B, Wu YX, Zhang SJ, et al. Morphine preconditioning confers cardioprotection in doxorubicin-induced failing rat hearts via ERK/ GSK-3beta pathway independent of PI3K/Akt. Toxicol Appl Pharmacol 2015;288:349–58. doi: <a href="https://doi.org/10.1016/j.taap.2015.08.007">https://doi.org/10.1016/j.taap.2015.08.007</a>.
- [39] Hong HJ, Liu JC, Chen PY, Chen JJ, Chan P, Cheng TH. Tanshinone IIa prevents doxorubicin-induced cardiomyocyte apoptosis through Akt-dependent pathway. Int J Cardiol 2012;157:174–9. doi: <a href="https://doi.org/10.1016/j.iicard.2010.12.012">https://doi.org/10.1016/j.iicard.2010.12.012</a>.
- [40] Lescoat A, Lelong M, Jeljeli M, Piquet-Pellorce C, Morzadec C, Ballerie A, et al. Combined anti-fibrotic and anti-inflammatory properties of JAK-inhibitors on macrophages in vitro and in vivo: perspectives for scleroderma-associated interstitial lung disease. Biochem Pharmacol 2020;178:114103.
- [41] Tavallai M, Booth L, Roberts JL, Poklepovic A, Dent P. Rationally repurposing ruxolitinib (jakafi ((r))) as a solid tumor therapeutic. Front Oncol 2016;6:142. doi: https://doi.org/10.3389/fonc.2016.00142.
- [42] Gallo S, Spilinga M, Albano R, Ferrauto G, Di Gregorio E, Casanova E, et al. Activation of the met receptor attenuates doxorubicin-induced cardiotoxicity in vivo and in vitro. Br J Pharmacol 2020;177:3107–22. doi: <a href="https://doi.org/10.1111/bph.15039">https://doi.org/10.1111/bph.15039</a>.
- [43] McBane JE, Santerre JP, Labow R. Effect of phorbol esters on the macrophage-mediated biodegradation of polyurethanes via protein kinase c activation and other pathways. J Biomater Sci Polym Ed 2009;20:437–53. doi: <a href="https://doi.org/10.1163/156856209X416467">https://doi.org/10.1163/156856209X416467</a>.
- [44] Chernov MV, Ramana CV, Adler VV, Stark GR. Stabilization and activation of p53 are regulated independently by different phosphorylation events. Proc Natl Acad Sci U S A 1998;95:2284–9. doi: <a href="https://doi.org/10.1073/pnas.95.5.2284">https://doi.org/10.1073/pnas.95.5.2284</a>.
- [45] Gyawali A, Krol S, Kang YS. Involvement of a novel organic cation transporter in paeonol transport across the blood-brain barrier. Biomol Ther (Seoul) 2019;27:290–301. doi: <a href="https://doi.org/10.4062/biomolther.2019.007">https://doi.org/10.4062/biomolther.2019.007</a>.
- [46] Farah CA, Sossin WS. The role of C2 domains in PKC signaling. Adv Exp Med Biol 2012;740:663–83. doi: <a href="https://doi.org/10.1007/978-94-007-2888-2">https://doi.org/10.1007/978-94-007-2888-2</a> 29.
- [47] Zhang L, Li DC, Liu LF. Paeonol: pharmacological effects and mechanisms of action. Int Immunopharmacol 2019;72:413–21. doi: <a href="https://doi.org/10.1016/j.intimp.2019.04.033">https://doi.org/10.1016/j.intimp.2019.04.033</a>.
- [48] Chen Xu, Zhang Z, Zhang X, Jia Z, Liu J, Chen X, et al. Paeonol attenuates heart failure induced by transverse aortic constriction via ERK1/2 signalling. Pharm Biol 2022;60(1):562–9.

- [49] Yarmohammadi F, Hayes AW, Karimi G. Natural compounds against cytotoxic drug-induced cardiotoxicity: a review on the involvement of PI3K/Akt signaling pathway. J Biochem Mol Toxicol 2021;35:. doi: <a href="https://doi.org/10.1002/jbt.22683">https://doi.org/10.1002/jbt.22683</a>e22683.
- [50] Rocca C, De Francesco EM, Pasqua T, Granieri MC, De Bartolo A, Gallo Cantafio ME, et al. Mitochondrial determinants of anti-cancer drug-induced cardiotoxicity. Biomedicines 2022;10(3):520.
- [51] Dong Q, Chen L, Lu Q, Sharma S, Li L, Morimoto S, et al. Quercetin attenuates doxorubicin cardiotoxicity by modulating Bmi-1 expression. Br J Pharmacol 2014:171(19):4440–54.
- [52] Octavia Y, Tocchetti CG, Gabrielson KL, Janssens S, Crijns HJ, Moens AL. Doxorubicin-induced cardiomyopathy: From molecular mechanisms to therapeutic strategies. J Mol Cell Cardiol 2012;52:1213–25. doi: <a href="https://doi.org/10.1016/j.yimcc.2012.03.006">https://doi.org/10.1016/j.yimcc.2012.03.006</a>.
- [53] Tang H, Tao A, Song J, Liu Q, Wang H, Rui T. Doxorubicin-induced cardiomyocyte apoptosis: Role of mitofusin 2. Int J Biochem Cell Biol 2017;88:55–9. doi: https://doi.org/10.1016/j.biocel.2017.05.006.
- [54] Wu X, Chen H, Chen X, Hu Z. Determination of paeonol in rat plasma by high-performance liquid chromatography and its application to pharmacokinetic studies following oral administration of moutan cortex decoction. Biomed Chromatogr 2003;17:504–8. doi: <a href="https://doi.org/10.1002/bmc.259">https://doi.org/10.1002/bmc.259</a>.
- [55] Vásquez-Trincado C, García-Carvajal I, Pennanen C, Parra V, Hill JA, Rothermel BA, et al. Mitochondrial dynamics, mitophagy and cardiovascular disease. J Physiol 2016;594(3):509–25.
- [56] Marques-Aleixo I, Santos-Alves E, Torrella JR, Oliveira PJ, Magalhaes J, Ascensao A. Exercise and doxorubicin treatment modulate cardiac mitochondrial quality control signaling. Cardiovasc Toxicol 2018;18:43–55. doi: https://doi.org/10.1007/s12012-017-9412-4.
- [57] Bowman T, Garcia R, Turkson J, Jove R. Stats in oncogenesis. Oncogene 2000;19:2474–88. doi: https://doi.org/10.1038/sj.onc.1203527.
- [58] Zhao J, Du J, Pan Y, Chen T, Zhao L, Zhu Y, et al. Activation of cardiac TrkB receptor by its small molecular agonist 7,8-dihydroxyflavone inhibits doxorubicin-induced cardiotoxicity via enhancing mitochondrial oxidative phosphorylation. Free Radic Biol Med 2019;130:557–67.
- [59] Gao J-L, Zhao J, Zhu H-B, Peng X, Zhu J-X, Ma M-H, et al. Characterizations of mitochondrial uncoupling induced by chemical mitochondrial uncouplers in cardiomyocytes. Free Radic Biol Med 2018;124:288–98.
- [60] Wang L, Zhang T-P, Zhang Y, Bi H-L, Guan X-M, Wang H-X, et al. Protection against doxorubicin-induced myocardial dysfunction in mice by cardiacspecific expression of carboxyl terminus of hsp70-interacting protein. Sci Rep 2016;6(1). doi: <a href="https://doi.org/10.1038/srep28399">https://doi.org/10.1038/srep28399</a>.
- [61] Catanzaro MP, Weiner A, Kaminaris A, Li C, Cai F, Zhao F, et al. Doxorubicininduced cardiomyocyte death is mediated by unchecked mitochondrial fission and mitophagy. FASEB J 2019;33(10):11096–108.
- [62] Hu X, Li S, Doycheva DM, Huang L, Lenahan C, Liu R, et al. Rh-CSF1 attenuates neuroinflammation via the CSF1R/PLG2/PKCepsilon pathway in a rat model of neonatal hie. J Neuroinflammation 2020;17:182. doi: <a href="https://doi.org/10.1186/s12974-020-01862-w">https://doi.org/10.1186/s12974-020-01862-w</a>.
- [63] Dorn 2nd GW, Souroujon MC, Liron T, Chen CH, Gray MO, Zhou HZ, et al. Sustained in vivo cardiac protection by a rationally designed peptide that causes epsilon protein kinase c translocation. Proc Natl Acad Sci U S A 1999;96:12798–803. doi: https://doi.org/10.1073/pnas.96.22.12798.
- [64] Hofmann PA, Israel M, Koseki Y, Laskin J, Gray J, Janik A, et al. N-benzyladriamycin-14-valerate (ad 198): A non-cardiotoxic anthracycline that is cardioprotective through PKC-epsilon activation. J Pharmacol Exp Ther 2007;323:658-64. doi: https://doi.org/10.1124/ipet.107.126110.
- [65] Xiong F, Xiao D, Zhang L. Norepinephrine causes epigenetic repression of PKCepsilon gene in rodent hearts by activating Nox1-dependent reactive oxygen species production. FASEB J 2012;26:2753-63. doi: <a href="https://doi.org/10.1096/fi.11-199422">https://doi.org/10.1096/fi.11-199422</a>
- [66] Ou Y, Li Q, Wang J, Li K, Zhou S. Antitumor and apoptosis induction effects of paeonol on mice bearing EMT6 breast carcinoma. Biomol Ther (Seoul) 2014;22:341–6. doi: https://doi.org/10.4062/biomolther.2013.106.
- [67] Fu J, Yu L, Luo J, Huo R, Zhu B. Paeonol induces the apoptosis of the SGC-7901 gastric cancer cell line by downregulating ERBB2 and inhibiting the NF-kappab signaling pathway. Int J Mol Med 2018;42:1473–83. doi: <a href="https://doi.org/10.3892/ijmm.2018.3704">https://doi.org/10.3892/ijmm.2018.3704</a>
- [68] Sun GP, Wang H, Xu SP, Shen YX, Wu Q, Chen ZD, et al. Anti-tumor effects of paeonol in a HepA-hepatoma bearing mouse model via induction of tumor cell apoptosis and stimulation of IL-2 and TNF-alpha production. Eur J Pharmacol 2008;584:246–52. doi: <a href="https://doi.org/10.1016/j.eiphar.2008.02.016">https://doi.org/10.1016/j.eiphar.2008.02.016</a>.